Reduced Transition between Open and Inactivated Channel States Underlies 5HT Increased I_{Na+} in Rat Nociceptors

Pablo d'Alcantara,* Luz M. Cardenas,† Stéphane Swillens,* and Reese S. Scroggs†
*I.R.I.B.H.N. and Laboratory of Neurophysiology, School of Medicine, Université Libre de Bruxelles, B-1070 Brussels, Belgium; and †University of Tennessee, Health Science Center, Department of Anatomy and Neurobiology, Memphis, Tennessee 38163 USA

ABSTRACT We previously demonstrated that activation of a $5HT_4$ receptor coupled cAMP-dependent signaling pathway increases tetrodotoxin-resistant Na^+ current (I_{Na}) in a nociceptor-like subpopulation of rat dorsal root ganglion cells (type 2). In the present study we used electrophysiology experiments and computer modeling studies to explore the mechanism(s) underlying the increase of I_{Na} by 5HT. In electrophysiological experiments with type 2 dorsal root ganglion cells, 5HT increased peak I_{Na} and the activation and inactivation rate, without significantly affecting the voltage dependency of activation or availability. Studies on the voltage dependency of channel availability, time course of removal of inactivation, and inactivation of evoked Na^+ currents suggested that there are at least two inactivation states of the Na^+ channel, one (I_{fast}) that is induced and retrieved faster than the other (I_{slow}). Long (1 s), but not short (60 or 100 ms), inactivating conditioning pulses (CPs) suppressed the 5HT-induced increase in I_{Na}. Computer modeling studies suggest that 5HT increased I_{Na} mainly by decreasing the transition rate (k_{OI1}) from an open state to I_{fast}. Furthermore, 5HT increased I_{Na} activation and inactivation rates mainly by increasing the transition rate from closed to open (k_{C3O}) and from I_{fast} to I_{slow} (k_{I1I2}), respectively. The antagonism of the 5HT-induced increase in I_{Na} by 1-s inactivation CPs may be due an enhancement of transitions from I_{fast} to I_{slow}, via the increase in k_{I1I2}. This may deplete the pool of channels residing in I_{fast}, reducing the frequency of reopenings from I_{fast}, which offsets the increase in I_{Na} produced by the reduction in k_{OI1}. The above findings fit well with previous studies showing that activation of the cAMP/PKA cascade simultaneously increases voltage sensitive tetrodotoxin-resistant Na^+ conductance and inactivation rate in nociceptors. The antagonism of the effects of 5HT by long inactivation CPs suggests that drugs designed to induce and/or stabilize the I_{slow} state might be useful for reducing hyperalgesia produced by inflammatory mediators.

INTRODUCTION

Previous studies have demonstrated that the hyperalgesia produced by 5HT and other inflammatory mediators involves protein kinase A (PKA)-mediated phosphorylation of tetrodotoxin (TTX)-resistant Na^+ channels (Cardenas et al., 2001; Taiwo et al., 1992; Taiwo and Levine, 1992: England et al., 1996; Gold et al., 1996, 1998; Fitzgerald et al., 1999). However, the changes in Na^+ channel function leading to increased nociceptor excitability have not been conclusively determined. England et al. (1996) proposed that the majority of the excitatory effect of PGE_2 on cultured neonatal sensory neurons was produced by a shift in the voltage of activation of TTX-resistant channels to more hyperpolarized potentials. Other studies found similar hyperpolarizing shifts in voltage of activation but also consistently observed large increases in peak Na^+ conductance (Gold et al., 1996, 1998; Fitzgerald et al., 1999).

To further investigate this question, we used electrophysiological experiments in a subpopulation of nociceptor-like dorsal root ganglion (DRG) cells (type 2), in which we previously demonstrated that activation of $5HT_4$ receptors coupled to a cAMP-dependent signaling pathway produces an increase in TTX-resistant Na^+ currents (Cardenas et al., 1995, 1997, 2001). The type 2 DRG cells consistently express several characteristics of nociceptors including small diameter cell bodies, long duration action potentials, TTX-resistant Na^+ current, and sensitivity to capsaicin (Cardenas et al., 1995, 1997; Harper and Lawson, 1985a,b; Holzer, 1991; Villiere and McLachlan, 1996). They also express a carbohydrate surface antigen (Galβ1–4 GlcNAc-R), previously associated with a subpopulation of DRG sensory neurons terminating in the substantia gelatinosa (Del Mar and Scroggs 1996; Dodd and Jessell, 1985; Light and Perl, 1976, 1979).

The studies presented below suggest that in this subpopulation of acutely isolated DRG cells, 5HT increases TTX-resistant Na^+ conductance and current activation and inactivation rate, whereas the voltage dependency of activation and channel availability is little affected. In addition, studies on the voltage dependency of Na^+ current availability, time course of retrieval from inactivation, and inactivation of evoked currents suggest the presence of at least two inactivated states: one that is induced and retrieved rapidly (I_{fast}) and another that is induced and retrieved more slowly (I_{slow}).

To probe possible mechanisms underlying the 5HT induced increase in Na^+ conductance, 40-ms Na^+ current

Submitted March 2, 2001, and accepted for publication March 29, 2002.
Address reprint requests to Reese Scroggs, Department of Anatomy and Neurobiology, University of Tennessee, Health Science Center, 855 Monroe Avenue, Memphis, TN 38163. Tel.: 901-448-7469; Fax: 901-448-9173; E-mail: rscroggs@nb.utmen.edu.
© 2002 by the Biophysical Society
0006-3495/02/07/05/17 $2.00

sweeps recorded before and after treatment with 5HT were fit with a minimal Na^+ channel gating model:

$$C_1 \xrightarrow{k_{CO}} C_2 \xrightarrow{k_{CO}} C_3 \underset{k_{OC}}{\overset{k_{CO}}{\rightleftharpoons}} O \underset{k_{I1O}}{\overset{k_{OI1}}{\rightleftharpoons}} I_1 \underset{k_{I2I1}}{\overset{k_{I1I2}}{\rightleftharpoons}} I_2$$

in which I_1 and I_2 correspond to I_{fast} and I_{slow}, respectively. These studies indicated that 5HT produced a significant decrease in k_{OI1} and a significant increase in k_{C3O} and k_{I1I2}. Subsequent computer simulations based on the above model, where k_{OI1}, k_{C3O}, and k_{I1I2} were changed individually, suggested that the 5HT induced increase in Na^+ conductance is primarily the result of a decrease in the rate of transition from the open state to I_{fast} (k_{OI1}). On the other hand, a 5HT induced increase in the transition from closed to open (k_{C3O}), and from I_{fast} to I_{slow} (k_{I1I2}) appeared to underlie the 5HT induced increases in the macroscopic activation and inactivation rates, respectively.

The increase in k_{I1I2} by 5HT may also underlie the antagonism of the 5HT induced increase in Na^+ current amplitude by long duration inactivation conditioning pulses (CPs). The increase in k_{I1I2} by 5HT may enhance the transition of channels from I_{fast} to I_{slow}, during the course of the long (1 s) inactivation CPs. This may deplete the pool of channels in I_{fast}, relative to that present after long inactivation CPs in the absence of 5HT. The resultant reduction in the reopening of channels from I_{fast} could offset the increase in Na^+ current amplitude via the 5HT-induced decrease in k_{OI1}.

The above findings fit well with previous studies showing that activation of the cAMP/PKA cascade simultaneously increases voltage sensitive TTX-resistant Na^+ conductance and Na^+ current activation and inactivation rate in nociceptors (Gold et al., 1996, 1998; Fitzgerald et al., 1999). Interestingly, another previous study suggested that PKA-dependent phosphorylation of TTX-sensitive Na^+ currents in rat striatal neurons, which decreases Na^+ conductance without affecting voltage of activation or inactivation, is associated with an increase in k_{OI1} (d'Alcantara et al., 1999). Thus, changes in the transition between Na^+ channel open and inactivated states may constitute a general mechanism by which Na^+ currents are modulated. Our data regarding the antagonism of the 5HT-induced increase in Na^+ current amplitude with long inactivation CPs suggests that development of drugs, which selectively induce or stabilize slow inactivation states of the TTX-insensitive Na^+ channel, could be useful in reducing the hyperalgesia produced by inflammatory mediators.

MATERIALS AND METHODS

Electrophysiology

Male rats (50–100 g), Sprague Dawley (purchased from Harlan) were rendered unconscious with methoxyflurane, decapitated, and DRG from lumbar and thoracic regions were dissected out. The ganglia were incubated at 36°C for 1/2 h in Tyrode's solution (composition below) containing: 1 mg/mL collagenase (Sigma, St. Louis, MO, Type 1A) and 2.5 mg/mL Dipase II (Roche, Basel, Switzerland). Individual DRG cell bodies were isolated by trituration and adhered to the bottom of a 35-mm petri dish, and superfused with Tyrode's solution containing: 140 mM NaCl, 4 mM KCl, 2 mM $MgCl_2$, 2 mM $CaCl_2$, 10 mM glucose, 10 mM HEPES, adjusted to pH 7.4 with NaOH.

All experiments were done at room temperature (23°C). Currents and voltages were recorded in the whole-cell patch configuration using an Axopatch 200A (Axon Instruments). Voltage commmands, and data acquisition and analysis were controlled using pClamp 8.0 (Axon Instruments, Union City, CA). Data were leak subtracted using the P/4 method. Electrodes were fabricated from soda lime capillary glass (Scientific Products, B4416-1) using a Narishige 2-stage vertical puller, coated with sylgard to ~200 μm from the tip, and fire polished to a final resistance of 0.8 to 2.0 MΩ, using a Narishige microforge. For voltage clamp experiments, series resistance was estimated from capacity transients after compensation, as described previously (Scroggs and Fox, 1992). No data were included where series resistance resulted in greater than a 10-mV error in voltage commands.

For most voltage clamp experiments on TTX-resistant Na^+ currents the patch electrodes were filled with a solution (internal solution) containing: 120 mM CsCl, 5 mM 2Na-ATP, 0.4 mM 2Li-GTP, 5 mM $MgCl_2$, 5 mM ethylene glycol-bis (β-aminoethylether)-*N*,*N*,*N*′,*N*′,-tetraacetic acid (EGTA), 1.86 $CaCl_2$, 20 (*N*-[2-hydroxyethyl]piperazine-*N*′-[2-ethanesulfonic acid]) (HEPES), adjusted to pH 7.4 with CsOH. Total $[Ca^{2+}]_i$ was calculated to be 100 nM. For isolation of Na^+ currents, the external solution contained: 50 mM NaCl, 112.5 mM tetraethylammonium chloride (TEA), 2 mM $CaCl_2$, 0.5 mM $CdCl_2$, 10 mM HEPES, and 0.0005 mM TTX, pH 7.4 with TEA-OH.

Additional internal and external solutions were used in experiments on Na^+ current activation designed to mimic conditions present in experiments of Rush et al. (1998) and Gold et al. (1996). For the Rush et al. (1998) conditions, the internal solution contained: 110 mM CsF, 5 mM $MgCl_2$, 10 mM NaCl, 11 mM EGTA, and 10 mM HEPES, pH 7.2 with CsOH. The external solution contained: 82.5 mM Choline-Cl, 20 mM TEA, 32.5 mM NaCl, 5 mM CsCl, 5 mM $MgCl_2$, 0.1 mM $CaCl_2$, 5 mM Glucose, 10 mM HEPES, 0.0005 mM TTX, pH 7.2 with NaOH. For the Gold et al. (1996) conditions, the internal solution contained: 140 mM CsCl, 6 mM NaCl, 4 mM $MgCl_2$, 0.1 mM $CaCl_2$, 11 mM EGTA, 10 mM HEPES, 2 mM 2Na+ATP, 1 mM 2Li+GTP, pH 7.2 with Tris-base. The external solution contained: 65 mM Choline-Cl, 40 mM TEA, 35 mM NaCl, 5 mM $MgCl_2$, 0.1 mM $CaCl_2$, 10 mM Glucose, 10 mM HEPES, 0.0005 mMTTX, pH 7.4 with NaOH. Solutions were changed around the cell under study by means of a small glass capillary tube placed near the cell in the bath as described earlier (Cardenas et al., 1997). Most chemicals and salts were obtained from Sigma. ATP and GTP were obtained from Boehringer Mannheim.

Experiments were restricted to type 2 DRG cells, which were identified (in Tyrode's solution) by the expression of an I_A-like current that was evoked upon repolarization to −50 mV after a 787-ms hyperpolarization to −90 to −110 mV (Cardenas et al., 1995, 1997). However, with Cs^+ replacing K^+ in the pipette solution to block K^+ currents, the A current was inward rather than outward. The data shown in the results section have not been corrected for liquid junction potential.

Estimation of voltage dependency of activation

The voltage where 1/2 of the Na^+ current was activated ($V_{1/2}$) was estimated from amplitudes of Na^+ currents evoked every 7 s by 40-ms test potentials to −55 mV through +50 mV (in 5-mV increments) from a holding potential of −60 mV. The peak current amplitudes observed at the different test potentials were converted to macroscopic conductance (g) using the relationship $g = I/(V_R - V_M)$, in which V_R is the apparent

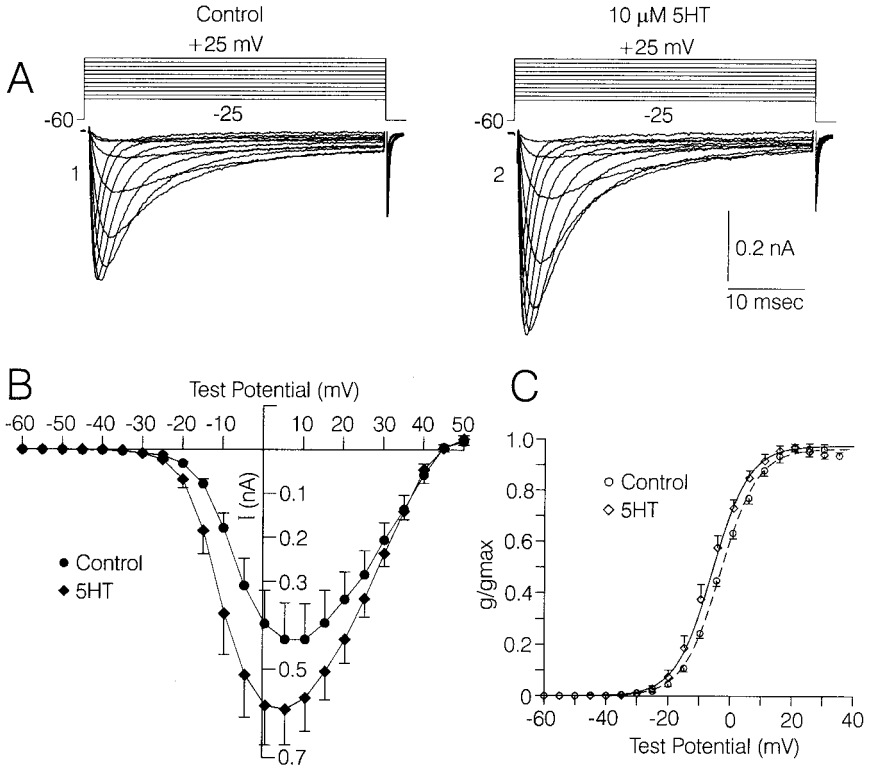

FIGURE 1 Effects of 5HT on the voltage dependency of activation of TTX-resistant Na^+ current in type 2 DRG cells. (*A*) Family of averaged Na^+ currents evoked with 40-ms depolarizations to voltages ranging from −25 mV to +25 mV, under control conditions (*1*) and after treatment with 10 μM 5HT (*2*). Each current record is the average from 11 experiments. The currents were recorded in the presence of 500 nM TTX. (*B*) Plot of current versus test potential, under control conditions (●) and after treatment with 5HT (◆). Each data point is the average of 11 experiments ± SE. (*C*) Plot of normalized macroscopic conductance versus voltage constructed from the data in *B* as described in the Materials and Methods. Each data point represents the average normalized conductance from 11 experiments ± SE. The line through the average data points represents the fit achieved with a Boltzmann function as described in the Materials and Methods. The values of $V_{1/2}$ and k for control and 5HT conditions generated by the Boltzmann fit to the average data points were similar to the corresponding average values of $V_{1/2}$ and k reported in the results. For *B* and *C*, the position of the data points along the x axis has been corrected for series resistance.

reversal potential of the Na^+ current in our system (≈ +45 mV), and V_M is the test potential. Best fit values for $V_{1/2}$ and the slope factor k were estimated by fitting the Boltzmann relationship: $g = g_{max}/(1 + \exp((V_{1/2t} - V_M)/k))$ to the macroscopic conductance observed at different test potentials, using a Gauss-Newton least squares iteration program (Systat, SPSS Inc.). For conversion from current to conductance, estimations of $V_{1/2}$, and plotting current-voltage and conductance-voltage relationships, all voltages were corrected for the effects of series resistance, which was measured from capacity transients recorded from each cell after series resistance compensation.

Estimation of voltage dependency of current availability

Availability curves were generated by giving 100-ms or 1-s conditioning potentials (CPs) to 0 mV through −140 mV or −120 mV, respectively, from a holding potential of −60 mV. Immediately after each CP, the DRG cells were given a test potential to +5 mV (peak current) to evaluate the amount of current available for activation. After each test pulse the leak was measured at the CP voltage and was subtracted from the preceding current using the P/4 method (P-Clamp, Axon Instruments). In between each cycle (consisting of CP + test pulse + leak) the cells were returned to the holding potential of −60 mV for 5 s (for graphical representation of the protocols see insets Fig. 3, *B* and *D*). The current amplitudes recorded from each cell were individually normalized relative to I_{max} observed in each cell, and fitted with a double Boltzmann function $I = f_1/(1 + \exp((V_M - V_{h1})/k_1)) + f_2/(1 + \exp((V_M - V_{h2})/k_2))$, in which the fitting parameters $f_1 + f_2 = I_{max} = 1$, and V_M = the CP potential. Best-fit values V_{h1} and V_{h2} and the slope factors (k_1 and k_2) were estimated using the Gauss-Newton least squares iteration program.

Estimation of the time course of removal of inactivation

Type 2 DRG cells, held at −80 mV, were given CPs to 0 mV, which alternated between 60 ms and 1 s in duration. No current was evoked by a test potential to +5 mV immediately after (no delay) either duration of inactivation pulse. To estimate the time course of removal of inactivation, the 60-ms and 1-s CPs were followed by repolarization to −80 mV for times ranging from 5 ms to 5 s (delay). Then after the various delays, test potentials to +5 mV were given to assess the recovery of the Na^+ current from inactivation (for a graphical representation of the protocol see the inset in Fig. 5 *B*). The cells were returned to the holding potential of −80 mV for 10 s between each cycle (which consisted of CP + delay + test pulse) to reset the channels. The current amplitudes recorded from each cell were individually normalized relative to I_{max} observed after a 5-s delay in each cell and were fit with a rising triple exponential function; $f_1 \times (1 - \exp(-t/\tau_1)) + f_2 \times (1 - \exp(-t/\tau_2)) + f_3 \times (1 - \exp(-t/\tau_3))$, in which the fitting parameters $f_1 + f_2 + f_3 = I_{max} = 1$ and t represents the delay period.

Computer modeling

The simulations and analyses with the models were made with the Matlab (The MathWorks, Inc.) software. Na^+ current traces obtained under control conditions and during the peak effect of 5HT were analyzed by curve fitting using a model describing the gating mechanism of the Na^+ channel as follows. The model, defined by kinetic transitions between different channel states (closed, open, or inactivated), was mathematically described by a system of first order differential equations:

$$\frac{dX_i}{dt} = \sum_{i \neq j}^{n} k_{ji} X_j - \sum_{i \neq j}^{n} k_{ij} X_i \qquad (1)$$

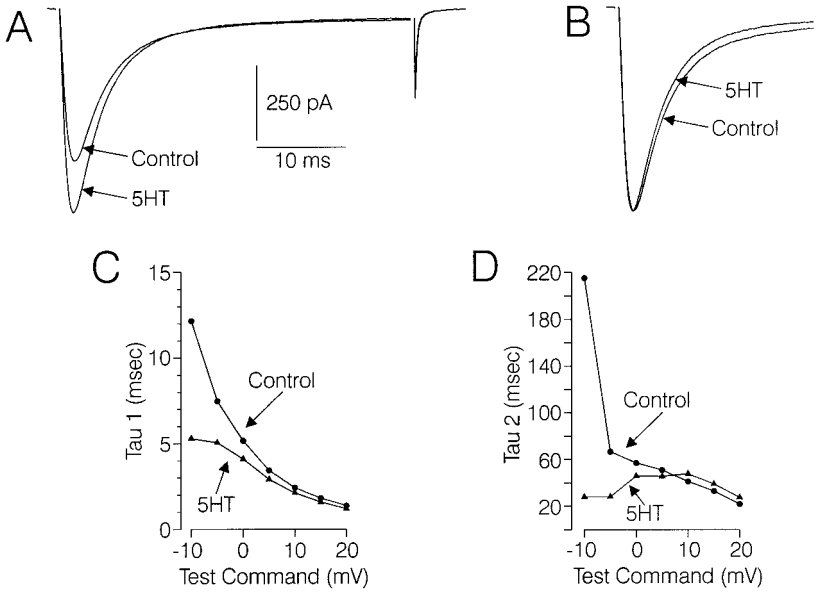

FIGURE 2 Effects of 5HT on macroscopic activation and inactivation rates of evoked TTX-resistant Na^+ currents. (*A*) Effects of 5HT on peak Na^+ current in 12 type 2 DRG cells used for analysis of macroscopic activation and inactivation rates. The current records corresponding to control conditions and 5HT treatment are each averages of current records from 12 experiments. In turn, each of the 12 current records included in the average control and 5HT sweeps, are averages of 5 to 10 individual currents recorded under control conditions or after treatment with 5HT. (*B*) Same current records as in *A*, except that the peak control current amplitude has been scaled up to match peak current amplitude observed after 5HT treatment. (*C* and *D*) Plots of τ_1 (*C*) and τ_2 (*D*) describing the macroscopic rates of Na^+ current inactivation, versus test potential used to evoke the Na^+ currents, under control conditions (●) and after treatment with 5HT (▲). Values of τ_1 and τ_2 were derived by fitting falling double exponential functions to the inactivating portion of the averaged current records shown in Fig. 1 *A*, corresponding to test commands of −10 mV through +20 mV.

in which X_i was the fraction of channel population in state *i*, and k_{ij} was the first order kinetic constant characterizing the conversion of state *i* to state *j*. These differential equations were numerically integrated by using the Runge-Kutta algorithm. This procedure gave the time course of the fraction of channel population in the open state, i.e., the open probability $p_o(t)$. To fit the model to the experimental data, the measured Na^+ current ($I(t)$) had to be numerically transformed into open probability, using the theoretical relationship:

$$I(t) = iNP_o(t) \quad (2)$$

in which *N* and *i* referred to the total number of channels and to the current of a single open channel, respectively. Practically, the value of the scaling factor *i N* could not be determined, because *N* was unknown in our experiments. To circumvent this problem, we referred to a study showing the voltage and time dependencies of the open probability of TTX-resistant Na^+ channels in frog DRG cells (Yakehiro et al., 2000) and assumed that, at a given test potential, the maximal open probability with respect to time ($p_{o,\,max}$) corresponded to the peak amplitude of Na^+ current (I_{max}). Thus, the following normalization was applied:

$$P_o(t) = I(t)/S \quad (3)$$

$$S = I_{max}/P_{o,max} \quad (4)$$

For example, the control current trace $I(t)$ (Fig. 6 *A*), which was obtained using a depolarization step from −60 mV to +5 mV, was transformed to the open probability $p_o(t)$ (Fig. 6 *B*) using a maximal open probability $p_{o,\,max}$ of 0.32. The calculation of this $p_{o,\,max}$ value was based on the Yakehiro et al. (2000) report, which determined from single channel studies that the maximal conductance for TTX-resistant Na^+ channels in frog DRG cells corresponded to an open probability of 0.4. The control current recorded from the type 2 DRG cell illustrated in Fig. 6 *A* was evoked using a depolarization to +5 mV, which corresponded to the voltage where 80% of the maximal conductance observed in this cell, as determined from a study of its current-voltage relationship. Thus, the $p_{o,\,max}$ of 0.32 for the peak of this current represents 80% of 0.4.

The kinetic parameters k_{ij} of the model were estimated by an iterative procedure searching for the set of parameter values generating the minimal deviation (least square fitting) between the experimental curve $p_o(t)$ and the theoretical curve given by numerical integration of the differential equations.

Statistical analysis was done using a two tailed paired *t*-test for comparison of pairs of responses observed in one group of cells. The student's *t*-test was used to make comparisons between mean responses from two different treatment groups. Also, analysis of variance was used in more complicated situations when two or more mean responses for a particular variable were to be compared between two treatment groups, and were likely influenced by two factors such as 5HT and voltage. All statistical analyses were carried out using Systat (SPSS Inc). The data in the results section are written as the mean ± SE.

RESULTS

Effect of 5HT on voltage of activation

Voltage of activation of TTX-resistant Na^+ currents in type 2 DRG cells was studied using different pipette and external solutions for comparison with analogous data collected in other laboratories. When using pipette and external solutions made up as per Rush et al. (1998) (see Materials and Methods), $V_{1/2}$ averaged −8.7 mV ± 2.9, the slope constant *k* averaged 7.7 ± 0.8, and g_{max} averaged 28.6 ± 10.1 nS ($n = 4$, data not shown). Similar values for $V_{1/2}$ (−10.3 mV ± 1.1), *k* (6.2 ± 0.3), and g_{max} (26.2 ± 5.3 nS) ($n = 9$, data not shown) were observed when the pipette and external solutions were switched to those used in a study by Gold et al. (1996) (see Materials and Methods). However, when Na^+ currents were recorded with the pipette and external solutions used throughout this study, $V_{1/2}$ averaged −0.3 ± 0.6 mV, *k* averaged 6.5 ± 0.4, and g_{max} averaged 13.6 ± 2.5 nS ($n = 11$) (Fig. 1, *B*, and *C*). The shift of $V_{1/2}$ in the depolarizing direction relative to values obtained using the solutions of Rush et al. (1998) or Gold et al. (1996) can be largely explained by the inclusion of 2 mM Ca^{2+} in our external solution to improve seal stability (Hille, 1992). Also, the smaller g_{max} observed in the present study may be attributed to the presence of 400 μM Cd^{2+}, which was

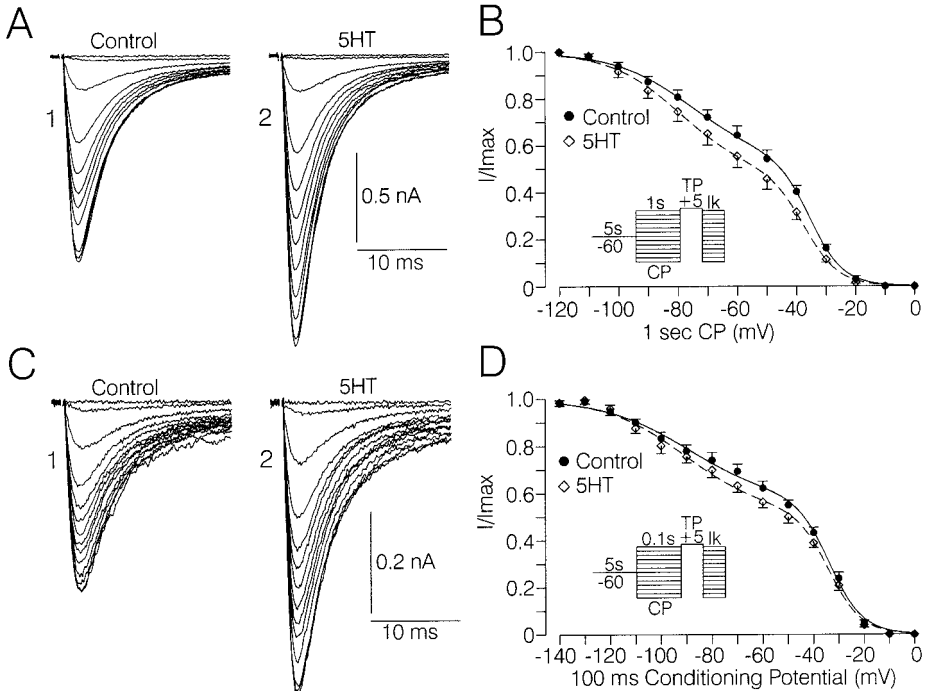

FIGURE 3 Effect of 5HT on the voltage dependency of availability of TTX-resistant Na^+ currents in type 2 DRG cells. (*A* and *C*) Na^+ currents evoked by a test potential to +5 mV after 1-s CPs to 0 mV through −120 mV (*A*) or 100-ms CPs to 0 mV through −140 (*C*), under control conditions (*1*), and after treatment with 5HT (*2*). The current records are averages from five experiments in *A* and six experiments in *C*. (*B* and *D*) Plot of average normalized current amplitude taken from (*A* or *C*), versus conditioning potential for control conditions (●) and after 5HT treatment (◇). For each cell included in *B* or *D*, the current was normalized to 1 relative to the largest current (I_{max}) observed through the range of CPs. The line passing through the averaged data points represents the fit to these points achieved with a double Boltzmann function as described in the methods. The values of V_h and k generated by fits to the averaged data points were similar to the average values of V_h and k generated by double Boltzmann fits to data from individual cells (Table 1). The insets in *B* and *D* are the protocols used to generate the currents in *A* and *C*, respectively, and are described in the Materials and Methods and text. The error bars represent the standard error of the mean.

included to block Ca^{2+} entry. At the concentration of 400 μM, Cd^{2+} could be expected to produce a partial blockade of TTX-resistant Na^+ channels (Akopian et al., 1996; Roy and Narahashi, 1992).

When the above mentioned 11 type 2 DRG cells were exposed to 10 μM 5HT peak Na^+ current was increased by 50 ± 9% from a control level of 438 ± 79 pA, to 614 ± 95 pA (Fig. 1, *A1* and *A2*). The maximal Na^+ conductance was increased 39 ± 9.0% by 5HT from the control level of 13.6 ± 2.5 nS to 17.3 ± 2.3 nS. After treatment with 5HT the $V_{1/2}$ for the conductance-voltage relationship was shifted by −2.9 ± 1.0 mV ($p = 0.005$, paired *t*-test), but the slope factor (k) was not significantly affected ($k = 6.5 \pm 0.4$ under control conditions and 5.9 ± 0.4 after treatment with 5HT) (Fig. 1 *C*). However, in five additional control type 2 DRG cells tested, $V_{1/2}$ was significantly shifted by −2.8 mV ± 0.7 mV as a result of waiting for ~5 min between control I-V curves ($p = 0.02$, paired *t*-test). The apparent reversal potential was also shifted by a similar amount. When $V_{1/2}$ observed after 5HT treatment was corrected individually for each of the 11 DRG cells, based on a drift rate of 0.0092 mV/s, the difference before and after 5HT treatment became +0.2 ± 1.2 mV. Thus, drift artifact could account for the change in $V_{1/2}$ observed before and after 5HT treatment. The gradual drift of the voltage of activation to more negative voltages was likely an artifact of the whole-cell patch configuration (Fernandez et al., 1984).

Effects of 5HT on the macroscopic rate of activation and inactivation of evoked Na^+ currents

In addition to increasing peak Na^+ current amplitude and conductance, 5HT also produced small but significant increases in the macroscopic rate of activation and inactivation. In the 12 experiments included, 10 μM 5HT increased peak Na^+ current by an average of 53 ± 9.6% (Fig. 2 *A*). The 5HT induced increase in inactivation rate became more apparent visually when the peak amplitudes of the control and 5HT current records were normalized (Fig. 2 *B*). Times to peak current and inactivation rate of peak current were analyzed in current records averaged from 5 to 10 individual 40-ms currents recorded before and after 5HT. Current segments, starting 1 to 3 ms after peak current to the end of the test potential, were fitted with falling exponential func-

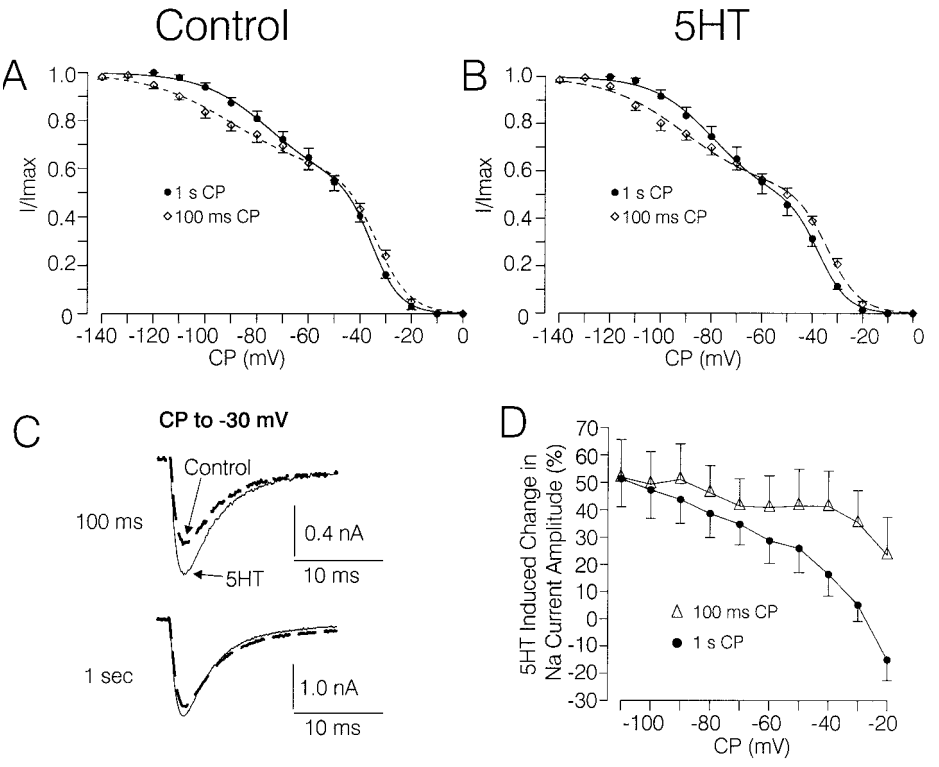

FIGURE 4 Effect of CP duration on Na^+ current availability and modulation by 5HT. (*A* and *B*) Comparison of availability curves generated with 1-s CPs versus 100-ms CPs, under control conditions (*A*) and after treatment with 5HT (*B*). (*C*) Test currents evoked under control conditions (*dashed line*) and after treatment with 5HT (*solid line*), after 100-ms and 1-s CPs to −30 mV. The current records corresponding to 1-s and 100-ms CPs are averages from five and six experiments, respectively. (*D*) Average 5HT induced changes in the amplitude of currents evoked after 100-ms conditioning potentials (△, $n = 6$) or after 1-s conditioning potentials (●, $n = 5$). The data for *A* to *D* was taken from the experiments depicted in Fig. 3, *A* to *D*. The error bars indicate the standard error of the mean.

tions. The data was not normalized nor changed in sign. A double exponential function [$a \times (\exp(-\text{time}/\tau_1)) + b \times (\exp(-\text{time}/\tau_2))$] gave better fits than single or triple exponential functions. Under control conditions, τ_1 averaged 4.22 ± 0.25 ms and was significantly reduced by 5HT to 3.76 ± 0.19 ms ($p = 0.0001$, paired *t*-test, $n = 12$). τ_2 was also significantly reduced by 5HT from 88.6 ± 14.1 ms under control conditions to 61.8 ± 9.8 ms after treatment with 5HT ($p = 0.03$, paired *t*-test). 5HT also produced a significant increase in the proportion of the fit associated with τ_1 from 71.6 ± 4.1% under control conditions to 78.2 ± 1.8% after treatment with 5HT ($p = 0.04$, paired *t*-test).

Double exponential functions were also fitted to the inactivating portion of the averaged current records shown in Fig. 1, *A1* and *A2* to analyze the effect of 5HT on the inactivation of Na^+ currents evoked by different test potentials. τ_1 decreased as test potential became more positive, as did the reduction in τ_1 produced by 5HT (Fig. 2 *C*). A similar pattern was observed for τ_2 (Fig. 2 *D*).

In addition to increasing inactivation rate, 5HT also produced a slight but significant increase in the activation rate of the Na^+ current, as judged by the time required for the current to peak (data not shown). In the same 12 cells depicted in Fig. 2 *A* and *B*, the current peaked 2.178 ± 0.082 ms after initiation of the test potential under control conditions, which was slightly but significantly later than the average time to peak of 2.066 ± 0.079 observed after treatment with 5HT ($p = 0.02$, paired *t*-test).

Effect of 5HT on Na^+ current availability

The effect of 5HT on the voltage dependency of availability of TTX-resistant Na^+ current was also studied in type 2 DRG cells. For these experiments the cells were given CPs to various voltages from a holding potential of −60 mV. After each CP and subsequent test potential, the cells were returned to −60 mV for 5 s to reset the channels (see insets, Fig. 3, *B* and *D*). Presumably CPs positive to −60 mV induced inactivation, whereas CPs negative to −60 mV removed inactivation.

In a group of six cells receiving 100-ms CPs, I_{max} averaged 379 ± 33 pA under control conditions and was increased to 578 ± 38 pA (56 ± 14%) after treatment with 5HT (Fig. 3, *A1* and *A2*). Similarly, in another group of five cells receiving 1-s CPs, 5HT increased I_{max} by 51 ± 9% from an average of 1141 ± 446 pA under control conditions to 1613 ± 551 pA after treatment with 5HT (Fig. 3, *C1* and *C2*). Control current amplitude, observed at −60 mV without a CP differed between the two groups to a similar degree as I_{max}. Thus, the difference in the average control I_{max} values between the two groups of cells appeared to be due mainly to sampling error rather than CP duration.

Availability curves were plotted individually for each of the cells receiving 100-ms or 1-s CPs (before and after 5HT), by plotting Na^+ current amplitude current (normalized to 1.0 relative to I_{max}) against conditioning potential (Fig. 3, *B* and *D*). The availability curves generated by either protocol appeared to be biphasic and were well fit by

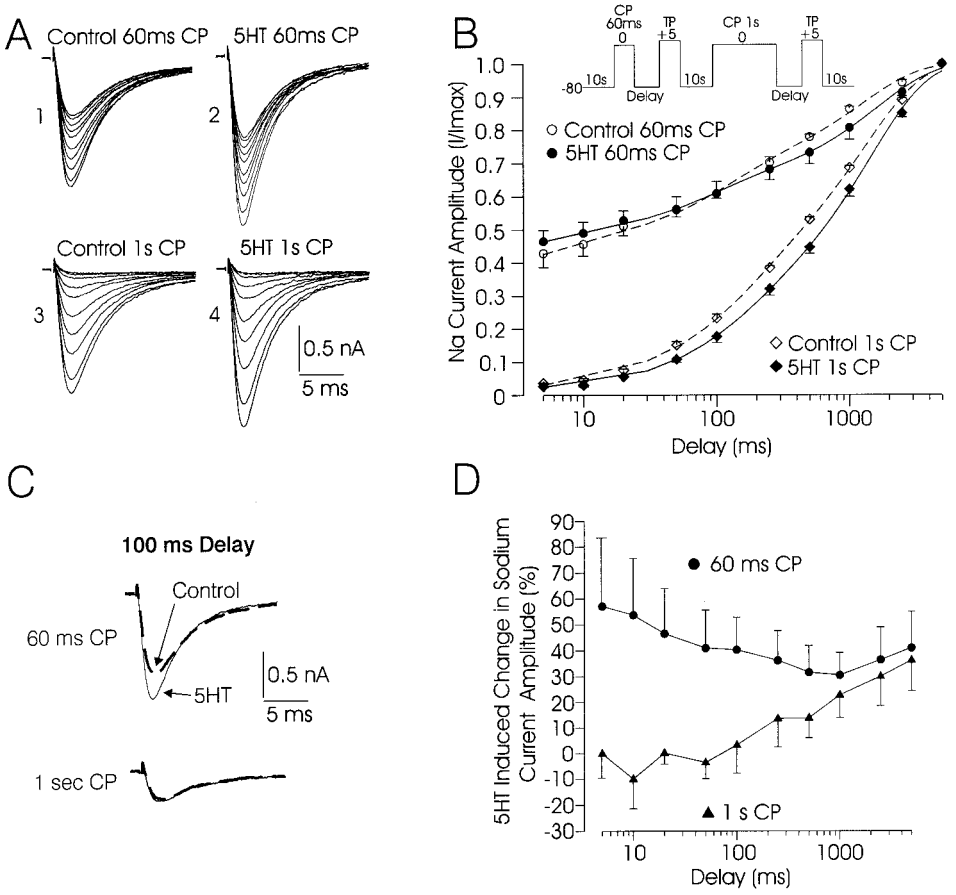

FIGURE 5 Effects of 60-ms and 1-s CPs on recovery from inactivation and modulation of Na^+ current amplitude by 5HT. (*A*) Currents evoked after delays of 5 ms to 5 s after 60-ms CPs under control conditions (*1*) and after treatment with 5HT (*2*), or after 1-s CPs under control conditions (*3*), and after treatment with 5HT (*4*). The currents are averages from four cells. (*B*) Plot of average normalized current amplitudes (taken from *B*) against delay time. The current amplitudes were normalized to 1 for each cell included, relative to the current observed at the 5-s delay (I_{max}). The open and closed circles represent control conditions and 5HT treatment, respectively for the 60-ms CPs, and the open and closed triangles represent control conditions and 5HT treatment, respectively for the 1-s CPs. The line through the average data points represents the fit to these points achieved with a triple exponential. The variables (τ and f) generated by fitting the triple exponential function to the averaged data points were similar to the average values of τ and f generated by triple exponential fits to data points in individual experiments. The inset is the protocol used to generate the currents from *A* and is described in the methods. Test currents evoked after a 100-ms delay under control conditions (*dashed line*) and after 5HT treatment (*solid line*), following a 60-ms CP (*upper panel*) or a 1-s CP (*lower panel*). Each current trace is the average of four experiments. (*D*) Effects of 5HT on Na^+ current amplitude at different delay times after 60-ms CPs (●) or 1-s CPs (▲). Each point represents the average from four experiments. The error bars indicate the standard error of the mean.

double Boltzmann functions. Treatment with 5HT did not significantly effect the voltage of Na^+ current availability, as judged by the estimates for V_{h1} and V_{h2} generated by the fitting procedure (Table 1). Also, the values obtained for the slope constant k were not changed significantly by 5HT (Table 1).

TABLE 1 Comparison of V_h, k, and f values for availability curves generated before and after 5HT with 100-ms and 1-s CPs

	Control		5HT	
	100-ms CP	1-s CP	100-ms CP	1-s CP
V_{h1}	−33.6 ± 1.1	−35.1 ± 0.8	−34.2 ± 1.2	−37.5 ± 0.5
k_1	6.3 ± 0.3	5.5 ± 0.2	6.5 ± 0.3	5.9 ± 0.5
f_1	0.562 ± 0.014	0.529 ± 0.040	0.521 ± 0.016	0.472 ± 0.027
V_{h2}	−87.8 ± 4.8	−75.2 ± 1.8	−90.3 ± 4.2	−78.5 ± 2.6
k_2	15.9 ± 0.7	12.6 ± 0.6	14.5 ± 1.2	11.6 ± 0.3
f_2	0.438 ± 0.014	0.471 ± 0.040	0.479 ± 0.016	0.528 ± 0.027

5HT did, however, produce a significant overall decrease in the normalized current amplitudes for both 100-ms and 1-s CPs (Fig. 1, *B* and *D*), which appeared to be most prevalent around the first shoulder of the availability curves corresponding to V_{h1} ($p = 0.001$ and 0.00004, respectively; 2-way analysis of variance (ANOVA) for 5HT effect with mV as the second factor). There was also a trend toward smaller values for the fitting parameter f_1 after treatment with 5HT, which possibly reflects the noticeable reduction in normalized current amplitude around V_{h1}. A decrease in f_1 after 5HT treatment was observed in four of the five cells given 1-s CPs and five of six cells given 100-ms CPs. However, this putative effect of

5HT did not reach significance, possibly due to the small sample sizes ($p = 0.095$ and 0.081 for 1-s and 100-ms CPs, respectively; paired *t*-test).

Effect of CP duration on Na^+ current availability

In contrast to 5HT treatment, variation in CP duration did have a significant effect on k and V_h values generated by Boltzmann fits to the availability curves (Fig. 4, *A* and *B*). Because values of V_h and k were not significantly affected by 5HT, the data for control and 5HT treated conditions were grouped for statistical analysis. The average k_1 and k_2 values associated with the 1-s pulses (5.7 ± 0.3 and 12.1 ± 0.4, respectively; $n = 10$) were significantly smaller than those (6.4 ± 0.2 and 15.2 ± 0.7, $n = 12$) associated with the 100-ms CPs ($p = 0.045$ and 0.001, respectively, Students *t*-test).

Values for V_{h1} and V_{h2} also differed significantly between the groups of cells given 1-s versus 100-ms CPs (Fig. 4, *A* and *B*). V_{h1} averaged −36.3 ± 0.6 mV ($n = 10$) for the 1-s CPs, which was significantly more negative than the average of −33.9 ± 0.8 mV ($n = 12$) for the 100-ms CPs ($p = 0.02$, Students *t*-test). V_{h2} averaged −76.8 ± 1.6 mV ($n = 10$) for the 1-s CPs, which was significantly more positive than the average of −89.0 ± 3.1 mV ($n = 12$) for the 100-ms CPs ($p = 0.003$, Students *t*-test).

Effect of CP duration on the modulation of the Na^+ current by 5HT

The increase in Na^+ current, usually observed after treatment with 5HT, was markedly antagonized by 1 s, but not 100-ms CPs, to depolarized potentials. As illustrated in Fig. 4 *C*, 5HT increased Na^+ current by 35 ± 12% after a 100-ms CP to −30 mV, which was similar to the 41 ± 12% increase in Na^+ current produced by 5HT in the absence of a 100 ms CP ($n = 6$). In contrast, 5HT increased Na^+ current by only 5 ± 6% after a 1-s CP to −30 mV, which was significantly less than the 29 ± 8% increase in Na^+ current produced by 5HT in the absence of a 1-s CP ($p = 0.02$, paired *t*-test; $n = 5$). The 5HT induced increase in Na^+ current amplitude was also reduced significantly more by 1-s CPs compared with 100-ms CPs, over the range of CP potentials from −110 mV to −20 mV (Fig. 6 *D*; $p = 0.0003$, 2-way ANOVA for CP duration with mV as the second factor).

Time course of removal of inactivation

In another series of experiments we studied the interaction of 5HT with the time course of removal of inactivation. For these experiments, type 2 DRG cells were given alternating 1-s and 60-ms CPs to 0 mV, which produced maximal inactivation. After various delay periods (5 ms–5 s), during which the membrane potential was returned to −80 mV, the amplitude of currents evoked by a command to +5 mV were recorded as a measure of how much inactivation had been removed. The cells were held at −80 mV for 10 s between each cycle of CP, delay, and test potential to reset the channels (see inset, Fig. 5 *B*).

TABLE 2 Comparison of τ and f values for removal of inactivation induced by 60-ms and 1-s CPs before and after 5HT

	Control, $n = 4$		5HT, $n = 4$	
	60-ms CP	1-s CP	60 ms CP	1 sec CP
τ_1	2.1 ± 0.3	1.5 ± 1.0	1.4 ± 0.5	2.0 ± 1.9
f_1	0.456 ± 0.031	0.024 ± 0.002*	0.480 ± 0.028	0.017 ± 0.006*
τ_2	108 ± 17	129 ± 13	84 ± 13	157 ± 29
f_2	0.213 ± 0.017	0.290 ± 0.008**	0.157 ± 0.015	0.226 ± 0.023**
τ_3	1237 ± 97	1,296 ± 20	1592 ± 75	1469 ± 53†
f_3	0.332 ± 0.018	0.686 ± 0.008**	0.364 ± 0.036	0.757 ± 0.019**

*Significantly less than for 60-ms CP, $p < 0.05$.
**Significantly greater than for 60-ms CP, $p < 0.05$.
†Significantly greater than control for 1-s CP, $p < 0.05$. Probabilities determined with a paired *t*-test.

After a 5-s delay after 60-ms CPs, the test current amplitude (I_{max}) averaged 1407 ± 453 pA under control conditions was increased to 1855 ± 444 pA (+41 ± 14%) after treatment with 5HT (Fig. 5, *A1* and *A2*). Current amplitude was reduced gradually by an average of ≈55% as the delay was shortened incrementally to the shortest time of 5 ms (Fig. 2, *A1* and *A2*). A somewhat different pattern was observed regarding 1-s CPs. 5HT increased I_{max} by +36 ± 12% (from 1354 ± 438 pA to 1736 ± 432 pA), similar to that observed regarding 60-ms CPs. However, I_{max} was reduced by ≈96% after a 5-ms delay (Fig. 5, *A3* and *A4*).

Plots of current amplitude (normalized to 1 relative to the peak amplitude observed with a delay of 5 s) versus delay were fitted with exponential functions to extract time constants for the rate of recovery (Fig. 5 *B*). The data was best fit by a triple exponential function. The average values for τ and the associated fitting parameters generated by individual fits for each of the four experiments are given in Table 2. In summary, the fitting procedure generated three distinct time constants (τ) in the proximity of 2, 100, and 1000 ms.

Effects of CP duration on the removal of inactivation

Varying the CP duration strongly affected the magnitude of the fitting parameters associated with the different time constants. The fitting parameter (f_1) associated with the fastest time constant (τ_1) was in the order of 50-fold smaller for the 1-s CPs versus the 60-ms CPs (Table 2). Conversely, the fitting parameters (f_2 and f_3) associated with the second and third time constants (τ_2 and τ_3) were ~40% and 100% larger, respectively, for the 1-s CPs versus the 60 ms CPs (Table 2). These effects of CP duration were significant under control conditions as well as after treatment with 5HT

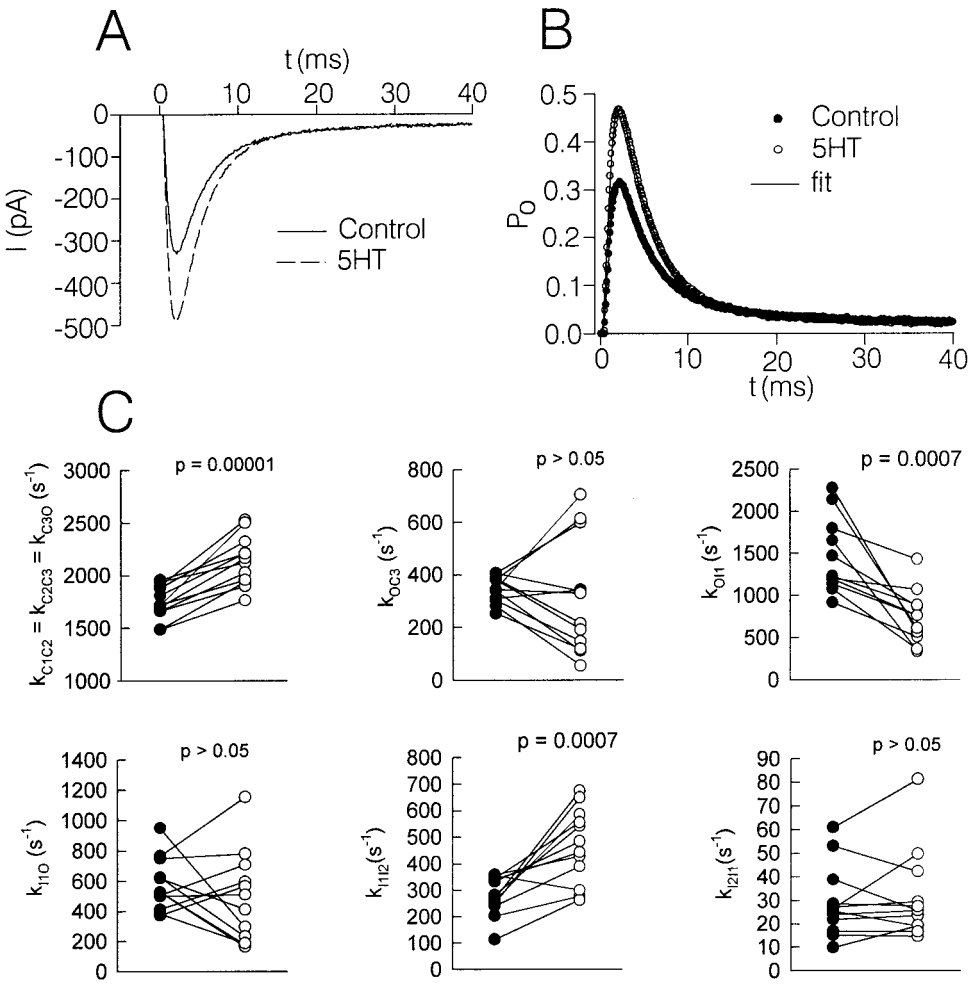

FIGURE 6 Effects of SHT on the estimates of kinetic rate constants for the transitions described in Model 2 using computer modeling of Na^+ current traces. (*A*) Representative current records showing the increase of TTX-resistant Na^+ current by 5HT in a type 2 DRG cell held at −60 mV and stepped to +5 mV. (*B*) Open probability time course was calculated using a scaling factor S = −1048 pA, and a line was fitted to the data according to Model 2 as described in the Materials and Methods. (*C*) Scatter plots of the kinetic parameters for 12 individual neurons with the following mean values under control conditions (●) and in the presence of 5HT (○), respectively: $k_{C1C2} = k_{C2C3} = k_{C3O} = 1744 \pm 46\ s^{-1}$ and $2137 \pm 68\ s^{-1}$, $k_{OC3} = 345 \pm 14\ s^{-1}$ and $314 \pm 63\ s^{-1}$, $k_{OI1} = 1441 \pm 126\ s^{-1}$ and $742 \pm 88\ s^{-1}$, $k_{I1O} = 579 \pm 50\ s^{-1}$ and $482 \pm 87\ s^{-1}$, $k_{I1I2} = 280 \pm 21\ s^{-1}$ and $466 \pm 41\ s^{-1}$, and $k_{I2I1} = 29 \pm 4\ s^{-1}$ and $31 \pm 5\ s^{-1}$. k_{CO} and k_{I1I2} were significantly increased, and k_{OI1} was significantly decreased in the presence of 5HT, whereas the other parameters were not changed significantly. Twelve current sweeps recorded under control conditions and after 5HT treatment (taken from the experiments depicted in Fig. 2 *A*) were used for modeling.

(paired *t*-test, $p = 0.02$ for f_2, control or 5HT, and $p = 0.0002$ for f_3, control or 5HT).

Effect of 5HT on the time course of removal of inactivation

Comparison of several parameters measured for control and 5HT treatment conditions suggest that 5HT slowed removal of inactivation. As illustrated in Fig. 5 *B*, 5HT produced an overall significant decrease in the normalized current amplitudes for 1-s CPs, but not for 60-ms CPs ($p = 2.2\ e^{-11}$ and 0.53, respectively; 2-way ANOVA for 5HT effect with delay as the second factor). There was also a trend toward increased values for τ_3 after treatment with 5HT that reached significance for the 1-s CPs, and approached significance for the 60-ms CPs (Table 2; paired *t*-test, $n = 4$, $p = 0.01$ and 0.07, respectively). The increase in τ_3 was accompanied by a larger fitting parameter (f_3), in four of four cases for the 1-s CPs and three of four cases for the 60-ms CPs. The change in f_3 approached statistical significance for the 1-s CPs ($p = 0.053$, paired *t*-test, $n = 4$).

Effect of CP duration on the modulation of the Na^+ current by 5HT

As with the above described availability experiments, modulation of Na^+ current by 5HT was significantly affected by CP duration. At the delay time of 100 ms after 60 ms CPs,

the Na^+ current was increased by an average of 40.3 ± 13% by 5HT, which was similar to that observed in the absence of a CP (39 ± 12.3%) (Fig. 5 *C*). In contrast, for the same delay after 1-s CPs, the Na^+ current was only increased by 3.3 ± 11%, which was significantly less than in the absence of a CP ($p = 0.02$, paired *t*-test, $n = 4$) (Fig. 5 *C*). Also, 1-s CPs significantly suppressed the 5HT induced increase in Na^+ current relative to that observed regarding 60-ms CPs, when all delay periods were grouped together (Fig. 5 *D*; $p = 0.000002$, 2-way ANOVA for 5HT effect with delay as second factor).

Computer modeling experiments

Computer modeling experiments were carried out to gain insight into possible mechanisms that could underlie the increase in TTX-resistant Na^+ current by 5HT. The current records from the 12 type 2 DRG cells depicted in Fig. 2 *A* were used for the computer modeling experiments. Various molecular models with different numbers of closed and inactivated states were tested for their ability to fit peak TTX-resistant Na^+ currents recorded from type 2 DRG cells held at −60 mV. The simplest model that provided a good fit consisted of three closed states, one open state, and two inactivated states (model 1). Models with fewer closed or inactivated states were not able to accommodate quantitatively the activation shapes of the 40-ms current records.

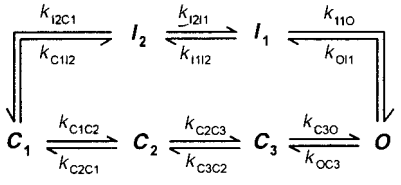

Model 1

When Model 1 was fitted to the experimental data, there appeared to be dependencies between the different kinetic parameters of the activation pathway and between the parameters of the two inactivation pathways. As in other studies (d'Alcantara et al., 1999), the dependencies were eliminated by simplifying the model; equating all the kinetic constants of the transitions leading to the open state ($k_{C1C2} = k_{C2C3} = k_{C3O}$) and neglecting the reverse transitions between closed states ($k_{C2C1} = k_{C3C2} = 0$). This hypothesis reflects the fact that the experimental data were not informative enough for estimating these constants individually.

Because of their mutual dependence, it was impossible to estimate the kinetic parameters of both inactivation pathways from a single experimental trace. However, the availability experiments suggested that 5HT did not significantly affect the voltage dependency of availability of TTX-resistant Na^+ channels in type 2 DRG cells (Fig. 3, Table 1). Because the principal objective was to identify the possible modifications of the gating mechanism responsible for an increase in Na^+ current, we removed the possibility of inactivation from the closed state in the model. The above manipulations led to the following operational model:

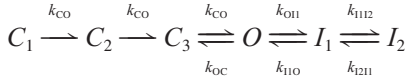

Model 2

To estimate the effects of 5HT on channel kinetics, $p_o(t)$ curves were generated for peak currents recorded under control conditions and in the presence of 5HT (holding potential −60 mV) for each of 12 type 2 DRG cells, using Eq. 3 as described in Materials and Methods (Fig. 6, *A* and *B*). Then the six unknown independent parameters were estimated for each cell under control conditions and during peak effect of 5HT by fitting the model to the $p_o(t)$ curves as described in the methods (Fig. 6 *B*).

The estimates of the six parameters, under control conditions and after treatment with 5HT, are summarized in Fig. 6 *C* for each of 12 cells. The parameters k_{C3O} and k_{I1I2} were both significantly increased by 23 ± 4% and 67 ± 15% from their control values ($p = 0.00001$ and 0.0007, respectively, paired *t*-test), and the parameter k_{OI1} was significantly decreased by 48 ± 6% of the control values ($p = 0.0007$, paired *t*-test). We did not detect a significant change in the other three parameters.

The effects of 5HT on k_{C3O}, k_{OI1}, and k_{I1I2} appeared to be reversible. In 8 of the 12 cells the Na^+ currents recorded following washout of the 5HT for an average of 10 min were again fitted to see if the effects of 5HT on the rate constants changed back toward control levels. In these eight cells, 5HT increased peak Na^+ current by 174 ± 31 pA (54 ± 14% increase), and the current was decreased by 245 ± 99 pA by the end of the washout period. Regarding these same eight cells, 5HT decreased k_{OI1} from a control level of 1317 ± 105 s^{-1} to 738 ± 125 s^{-1}, which returned to 1459 ± 211 s^{-1} over the washout period. k_{C3O} and k_{I1I2} averaged 1777 ± 55 s^{-1} and 280 ± 28 s^{-1}, under control conditions, respectively, were increased by 5HT to 2204 ± 77 s^{-1} and 486 ± 54 s^{-1}, and fell to 1804 ± 69 s^{-1} and 348 ± 26 s^{-1}, respectively over the washout period. For all three rate constants, the changes produced by 5HT as well as the changes produced by washout relative to 5HT conditions were significant ($p < 0.05$ for all, paired *t*-test with Bonferroni adjustment for multiple comparisons). On the other hand the values for k_{OC3}, k_{I1O}, and k_{I2I1} were not significantly affected by 5HT or washout relative to control conditions.

As illustrated in Figs. 1 *B* and 7, *A* and *B*, 5HT produced a much larger relative increase in Na^+ currents evoked with smaller test potentials compared with those evoked with

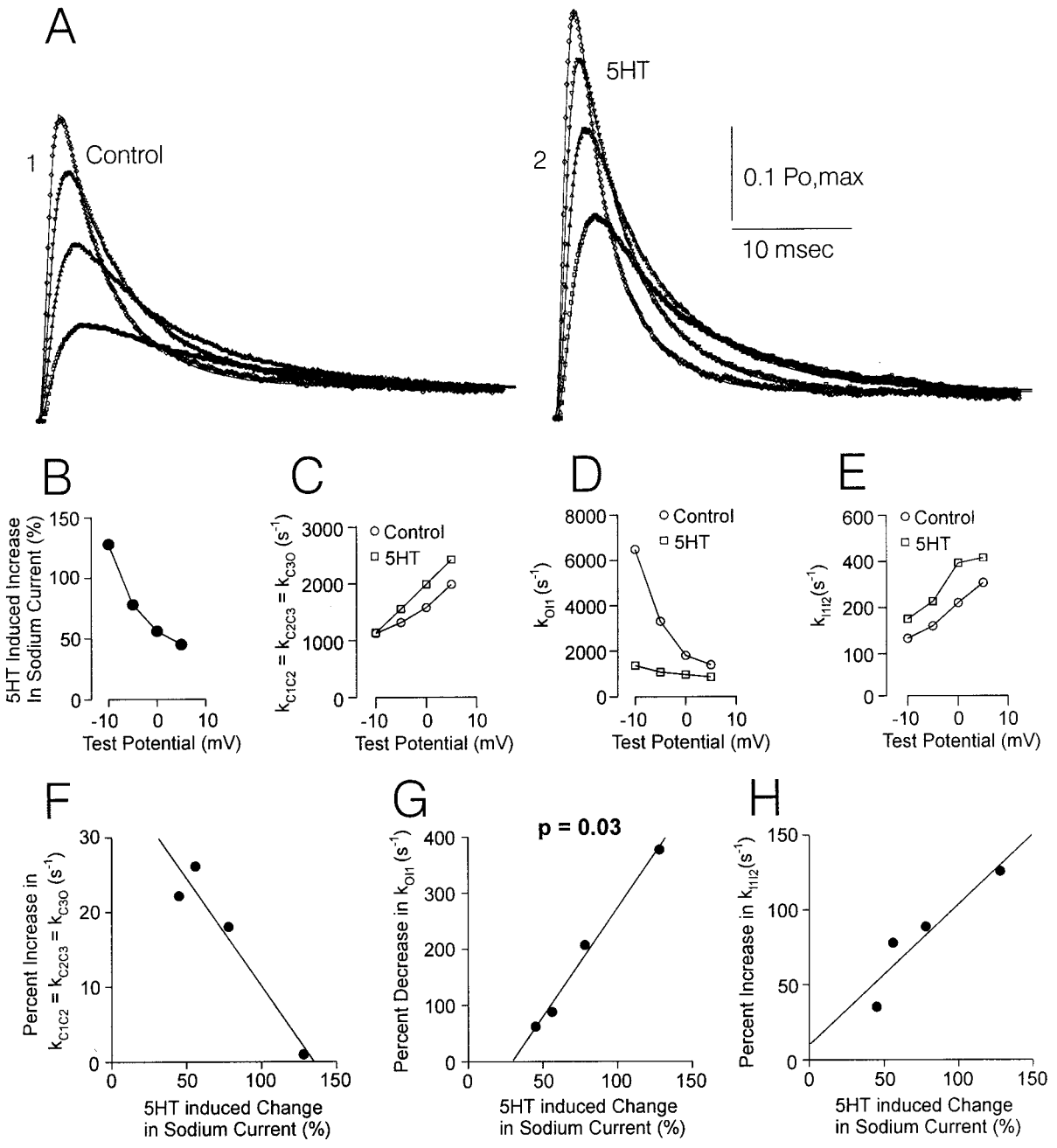

FIGURE 7 Effect of varying test potential on the 5HT induced changes in k_{C3O}, k_{OI1}, and k_{I1I2}. (*A*) Fit of Model 2 to Na^+ channel open probability for current records obtained using test potentials ranging from −10 mV to +5 mV. The corresponding averaged current records shown in Fig. 1, *A1* and *A2*, were used for transformation into open probability and fitting. The $p_{o,\,max}$ corresponding to each test potential under control conditions was derived from the averaged *g-V* plot shown in Fig. 1 *C*. (*B*) Percent increase in TTX-resistant Na^+ current produced by 5HT for different test potentials. (*C* to *E*) Estimates of k_{C3O}, k_{OI1}, and k_{I1I2} for different test potentials, under control conditions (*circles*) and after treatment with 5HT (*squares*). (*F–H*) Plots of percent change in k_{C3O}, k_{OI1}, and k_{I1I2} produced by 5HT versus percent increase in TTX-resistant Na^+ current produced by 5HT for different test potentials. Percent change in k_{OI1} was significantly correlated with percent change in Na^+ current produced by 5HT, whereas percent change in k_{C3O} and k_{I1I2} were not. Pearson correlation coefficients = 0.995, 0.960, 0.928, and p = 0.03, 0.24, 0.43, respectively for k_{OI1}, k_{C3O}, and k_{I1I2} (Bonferroni adjustment for multiple comparisons).

larger test potentials. Additional modeling experiments were carried out to see if the 5HT induced changes in k_{C3O}, k_{OI1}, and k_{I1I2} regarding peak Na^+ currents were conserved regarding currents evoked by different test potentials. As illustrated in Fig. 7, *A1* and *A2*, TTX-resistant Na^+ currents, which were evoked by different test potentials ranging from −10 mV to +5 mV, were well fit by Model 2, before and after treatment with 5HT. (For this modeling the averaged

TABLE 3 Comparison of TTX-resistant Na^+ currents expressed by type 2 DRG cells to three subtypes of TTX-resistant Na^+ currents proposed by Rush et al. (1998)

Activation	$V_{1/2}$	Type 2 DRG cell −16 mV*	TTX-R2 −17 mV**	TTX-R1 −8 mV**	TTX-R3 −36 mV
Availability (1 sec CP)	V_{h1}	−52 mV†	−46 mV	−29 mV	−68 mV
	k_1	5.5	3.8	3.1	5.8
	f_1	0.53	0.74	0.92	0.56
	V_{h2}	−92 mV†	−75 mV	−48 mV	−116 mV
	k_2	12.6	12.0	12.1	9.8
	f_2	0.47	0.26	0.08	0.44
Retrieval from Inactivation	τ_1	3.5 ms	3.3 ms	1.6 ms	n.t.
(60 ms CP)‡	f_1	0.52	0.58	0.91	n.t.
	τ_2	679 ms	902 ms	908 ms	n.t.
	f_2	0.48	0.42	0.09	n.t.
Use-dependence at 1-Hz stim rate		I_{na} reduced −46% in 14 s	I_{na} reduced −46% in 20 s	I_{na} reduced −17% in 20 s	n.t.

All values reported for TTX-R1, TTX-R2, and TTX-R3 were obtained using solutions E3/I1 (Rush et al., 1998).
*Corrected −7 mV for junction potential.
**Corrected +4 mV for series resistance.
†Corrected −6.8 mV for junction potential, and −10 mV for a shift likely produced by 2 mM Ca^{2+} in the external solution.
‡Values of τ and f were generated by fitting of double exponential functions.
n.t., Not tested.

current records illustrated in Fig. 1 *A* were used.) However, for some other test potentials, the Model 2 did not fit well (see Discussion; data not shown). For these reasons, the effects of 5HT on the rate constants are presented below only for currents evoked by test potentials ranging from −10 mV to +5 mV.

For the most part, the changes in k_{C3O}, k_{OI1}, and k_{I1I2} produced by 5HT regarding peak Na^+ current (Fig. 6) were also observed regarding Na^+ currents evoked by smaller test potentials (Fig. 7, *C–E*). The 5HT-induced change in k_{OI1} appeared to most closely parallel the effects of 5HT on Na^+ current, becoming smaller as the amplitude of the test potential was increased (compare Fig. 7, *B* with *D*). The percent change in k_{OI1} produced by 5HT was significantly correlated with the percent change in Na^+ current produced by 5HT, whereas percent changes in k_{C3O} and k_{I1I2} were not (Fig. 7, *F–H*).

DISCUSSION

Electrophysiological studies

One the main goals of the present study was to better characterize the TTX-resistant Na^+ conductance expressed by type 2 DRG cells to facilitate comparisons with TTX-resistant Na^+ currents observed in other preparations. A comparison of the TTX-resistant Na^+ channel in type 2 DRG cells with the TTX-R1, TTX-R2, and TTX-R3 subtypes proposed by Rush et al. (1998) is presented in Table 3. The voltage dependency of activation of the TTX-resistant Na^+ current in type 2 DRG cells was carried out in the same solutions used in the Rush et al. (1998) study. Given corrections to our data for junction potential (−7 mV) and corrections to the data of Rush et al. (1998) for series resistance (+4 mV, their estimate), the $V_{1/2}$ of activation for TTX-resistant Na^+ current in type 2 DRG cells most closely matches that of the TTX-R2 subtype (Table 3).

We studied the availability of the TTX-resistant Na^+ current in type 2 DRG cells using a voltage command protocol identical to that used by Rush et al. (1998), but using different internal and external solutions that reduced rundown and improved seal stability in our system. Given corrections to our data for junction potential (−6.8 mV) and for the presence of 2 mM Ca^{2+} in our external solution (−10 mV), the V_{h1} and V_{h2} values we observed regarding availability most closely resembled those of the TTX-R2 channel (Table 3). In addition we observed biphasic availability curves similar to those reported for TTX-R2 subtype in the Rush et al. (1998) study, where a significant proportion of the fit was associated with the more negative V_{h2}. In contrast the TTX-R1 subtype exhibited availability curves that appeared mostly monophasic, and when fit with double Boltzmann functions, over 90% of the fit was associated with the more depolarized V_{h1} (Table 3).

Our data regarding removal of inactivation also suggests that type 2 DRG cells express the TTX-R2 Na^+ channel. As described in the results section, we observed that triple exponential functions fit the time course of removal of inactivation better than the double exponential functions used by Rush et al. (1998). On the other hand, when we fit our data with double exponential functions we got fast and slow time constants very similar in magnitude to those observed by Rush et al. (1998) for the TTX-R2 channel (Table 3). Furthermore over 50% of the overall fit was attributed to the slow time constant, similar to the scenario

observed for the TTX-R2 channel (Table 3). In contrast, removal of inactivation from the TTX-R1 channel could be explained mostly by a rapid rate of retrieval (Table 3).

A final observation is that both the TTX-resistant Na^+ current in type 2 DRG cells and the TTX-R2 subtype exhibit pronounced use-dependence, in contrast to the TTX-R1 subtype (Table 3). The term "use-dependence" was coined by Rush et al. (1998) to stand for the decrease in peak Na^+ current amplitude produced by evoking peak Na^+ currents at a rate of 1 Hz. As illustrated in Table 3, the TTX-R2 subtype and the TTX-resistant Na^+ current expressed by type 2 DRG cells exhibit pronounced use-dependence, whereas this phenomena is seen to a much lesser degree regarding the TTX-R1 subtype (Cardenas et al., 2001; Rush et al., 1998).

Several observations suggest the existence of multiple inactivation states of the TTX-resistant Na^+ channel in type 2 DRG cells. The observation that a double exponential function was required to fit the inactivation of evoked Na^+ currents fits with the idea of multiple inactivated states. The different time constants describing this inactivation may reflect transitions from the open state to different inactivation states. Also, the observation that the availability curves were biphasic suggests the possibility of multiple inactivation states. One possibility is that the values of V_{h1} and $V_{h2,}$ generated when fitting double Boltzmann functions to the data, represent ½ inactivation for one inactivation state versus another, although there could be other interpretations. A third piece of evidence is the observation of three rates of removal of inactivation, which may correspond to transitions from different inactivation states to closed states.

More specifically, several additional observations suggest the hypothesis that there are two inactivation states, one (I_{fast}) that is induced and retrieved faster than the other (I_{slow}). As mentioned above, evoked Na^+ currents inactivated according to two time constants averaging ≈3 ms and 88 ms. The more rapid time constant may reflect the transition from the open state to an initial inactivation state, which in conformational terms, is closest to the open state. The slower time constant may reflect a slower transition from the initial inactivation state to a subsequent inactivation state, which is farther from the open state.

The steeper availability curves generated with long versus short CPs also fits with the hypothesis of I_{fast} and I_{slow} states. For submaximal potentials, the 1-s CPs could be expected to induce and retrieve more channels to and from the inactivated state, due to the additional time available for transitions to and from I_{slow}. The result of this would be steeper curves both for induction and retrieval of inactivation.

Varying CP duration had significant effects on V_{h1} and V_{h2}, in the availability experiments, which can also be explained in terms of I_{slow} and I_{fast}. Due to more time available for transitions to I_{slow}, V_{h1} could be expected to be more negative for 1-s CPs because less positive voltages would be required to induce the inactivated state in ½ of the channels not already inactivated at the holding potential of −60 mV. Similarly, due to more time available for transitions from I_{slow} to closed, V_{h2} could be expected to be more positive for 1-s CPs because less negative voltages would be required to remove inactivation from ½ of the channels that are inactivated at −60 mV.

The effects of CP duration on fitting parameters in the removal of inactivation experiments also fit with the hypothesis of I_{fast} and I_{slow}. In these experiments, the fitting parameters associated with the three time constants describing removal of inactivation, represent the proportion of the total fit attributed to each time constant. Thus, based on fitting parameter values, 1-s CPs (compared with 60-ms CPs) induced dramatically less inactivation than was removed according with the fastest time constant, and significantly more inactivation than was removed according to the two slower time constants (Table 2). One interpretation of this could be that the 1-s CPs initially induced a greater number of channels into I_{slow}, which was removed according to the slower time constants.

Thus, the hypothesis that fits the data best overall is that there are two inactivated states, I_{fast} and I_{slow}, illustrated below in Model 3:

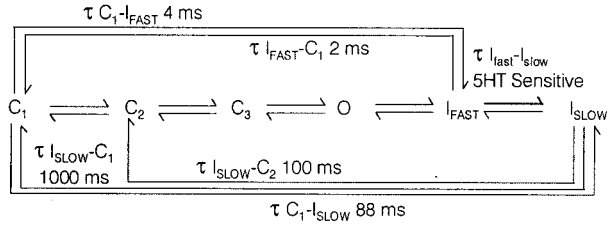

Model 3

Model 3 holds that I_{fast} is induced and retrieved rapidly with time constants in the proximity of 2 to 4 ms. On the other hand, I_{slow} is induced with a time constant averaging 88 ms for depolarizations that evoke peak Na^+ current, and is retrieved according to two time constants in the proximity of 100 ms and 1 s. The two time constants for retrieval of I_{slow}, could possibly represent transitions from I_{slow} to different closed states. The time constants for induction and retrieval of I_{fast} and I_{slow} in Model 3 are based on the inactivation of evoked Na^+ currents and the removal of inactivation experiments and on the assumption that the rates of induction of I_{fast} and I_{slow} from the closed state resemble their rates of induction from the open state. They are meant to be theoretical approximations only. The assumption that I_{slow} is retrieved to different closed states (not necessarily C_1 and C_2) is based on earlier work indicating that multiple rates of retrieval from inactivation can represent transitions from one inactivation state to different closed states (Vandenberg and Bezanilla, 1991; Goldman, 1995).

The hypothetical scenario that I_{slow} undergoes transitions to different closed states was adopted solely to match up our

observations that two time constants best described inactivation of evoked Na^+ currents, whereas three time constants best described removal of inactivation. Other scenarios could serve this purpose equally well, such as hypothesizing that I_{fast} undergoes transitions to different closed states. In any case, the observation of three time constants in the removal of inactivation experiments suggests an alternate hypothesis: there are three inactivation states, possibly exhibiting fast, intermediate, and slow rates of induction and retrieval. However, if this were the case, one might expect to find a third slow component of inactivation in the records of evoked Na^+ currents, that corresponds to the slowest time constant for removal of inactivation. Such a slow component was not detected in the Na^+ current records, despite much effort in this behalf. In addition, the previous work of Vandenberg and Bezanilla (1991) and Goldman (1995) suggest that different time constants for retrieval do not necessarily correspond to distinct inactivation states.

The characteristics of the inactivation states incorporated into Model 3 fit with the phenomenon of use-dependence first described by Rush et al. (1998). As mentioned above, the term "use-dependence" was applied by Rush et al. (1998) to describe the rapid decline in TTX-R2 Na^+ current amplitude that occurs when peak Na^+ currents are evoked at a rate of 1 Hz using 30-ms-long test potentials. We have observed a similar degree and rate of use-dependence regarding the TTX-resistant Na^+ currents in type 2 DRG cells (Cardenas et al., 2001). Use-dependence could be explained by induction, during the 30-ms test potentials, of a slowly retrieved form of inactivation. This inactivation could accumulate over the course of a 1-Hz train if it were not completely removed during the 1-s interpulse interval, resulting in a progressive decrease in current amplitude (Rush et al., 1998). The I_{slow} proposed in Model 3 has characteristics that could be expected to result in use-dependence, i.e., inducible by a 30-ms test potential, yet not completely removed within 1 s.

Computer modeling studies

A second major goal of the present study was to examine potential mechanisms that could underlie the 5HT-induced increase in TTX-resistant Na^+ current amplitude in type 2 DRG cells. For this purpose we initially developed a model depicting theoretical states of the TTX-resistant Na^+ channel in type 2 DRG cells (Model 2), which was the simplest model that closely fit peak Na^+ currents evoked by test potentials to 0 or +5 mV. Subsequently we observed that Model 2 closely fit Na^+ currents evoked by test potentials ranging from −10 mV to +5 mV, before and after treatment with 5HT (Fig. 7 *A*). However, for currents evoked by test potentials outside this range, the fit provided by Model 2 deviated noticeably from the peaks and/or the inactivating portions of the open probability curves. These deviations from a good fit for test potentials outside the −10 mV to +5 mV range might result from induction of additional channel states not included in Model 2 or failure to induce channel states that are included in Model 2. For test potentials more positive than +5 mV, a model with less closed states and more inactivation states might better account for the relatively high maximal conductances and rapid inactivation rates. For test potentials negative to −10 mV, a model with fewer inactivation states might better account for the relatively slow inactivation or complete lack of inactivation occurring over the 40-ms records.

When restricted based on the above caveats, application of Model 2 to Na^+ currents recorded before and after 5HT suggested changes in channel gating kinetics that fit well with our electrophysiological observations. Theoretically, the increase in Na^+ current by 5HT could be due to changes in three basic properties of the channels that are given by Eq. 2; i, N, and $p_o(t)$. One possibility is that 5HT could increase the total number of channels (N) by insertion of new channels into the membrane or shifting the voltage dependency of channel availability to more positive potentials. Alternatively, 5HT might increase the single channel ionic conductance (i) and/or alter the kinetic gating of the channels ($p_o(t)$).

The possibility that 5HT might increase (N) or (i) does not fit well with the available data. As reported in the results, 5HT did not shift the voltage dependency of channel availability to more positive potentials. Also, we observed that 5HT increased the macroscopic activation and inactivation rate (Fig. 2 *B*). Similar changes in macroscopic activation and inactivation rate of TTX-resistant Na^+ current have been observed in previous studies on inflammatory mediators and pharmacological agents, which increase cAMP, similar to $5HT_4$ receptor activation in type 2 DRG cells (Cardenas et al., 1997, 2001; Gold et al., 1996, 1998). These observations do not fit well with the idea that 5HT increased the voltage dependent Na^+ current peak by inserting new channels into the membrane (N) or increasing the single channel conductance (i). If the increase in Na^+ conductance by 5HT were due exclusively to an increase in the number of channels and/or the single channel conductance, we would expect a purely proportional increase in current amplitude without changes in macroscopic activation or inactivation rate.

Thus, at present, the most attractive hypothesis is that 5HT increased the TTX-resistant Na^+ current amplitude and conductance by altering channel-gating kinetics ($p_o(t)$). This hypothesis is supported by the results of our modeling: that 5HT increased the rates of transition from the closed state to the open state (k_{C3O}) and from I_{fast} to I_{slow} (k_{I1I2}), and decreased the rate of transition from the open state to I_{fast} (k_{OI1}).

To get a better idea regarding which effects of 5HT on current shape were associated with changes in k_{C3O}, k_{OI1}, or k_{I1I2}, computer simulations of TTX-resistant Na^+ currents were carried out. In these simulations k_{C3O}, k_{OI1}, and k_{I1I2}

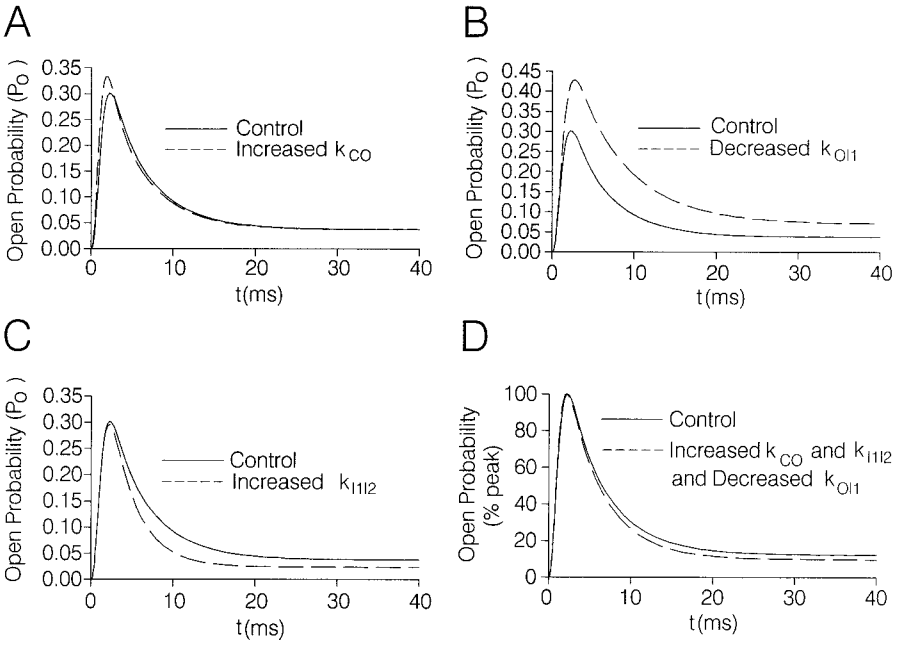

FIGURE 8 Effects on simulated Na^+ current shape of changing k_{C3O}, k_{OI1}, and k_{I1I2} individually from control values to values observed after treatment with 5HT in real experiments. (*A*) Effects of a 23% increase in k_{CO} on the simulation of open probability. (*B*) Effects of a 48% decrease in k_{OI1} on the simulation of the open probability. (*C*) Effects of a 68% increase in k_{I1I2} on the simulation of open probability. (*D*) Effects of increasing k_{CO} and k_{I1I2} by 23% and 68%, respectively, and decreasing k_{OI1} by 48%, on the simulation of open probability. In *D*, the simulated currents have been normalized to 100% of the peak current corresponding to 5HT conditions to facilitate visual comparison of inactivation rates. For *A* to *D* the kinetic parameters under control and 5HT conditions were taken from the mean values inserted in the legend of Fig. 6.

were changed one at a time from the average control value to the average value observed in the presence of 5HT, whereas the other parameters were held constant at control levels (Fig. 8, *A–C*). These simulations suggest that the slight increase in activation rate and a small part of the increase in amplitude observed in the electrophysiological experiments were due to the 5HT-induced increase of k_{C3O} (Fig. 8 *A*). However, most of the increase in Na^+ current amplitude produced by 5HT seems to be best explained by a decrease in k_{OI1} (Fig. 8 *B*). This latter conclusion is further supported by the observation that the percent change in k_{OI1} produced by 5HT for different test potentials was significantly correlated with the corresponding percent change in Na^+ current amplitude produced by 5HT (Fig. 7, *D* and *G*).

Regarding inactivation, the simulations suggest that the decrease in k_{OI1} decreased the macroscopic inactivation rate (Fig. 8 *B*). However, this was overcompensated by a larger increase in the macroscopic inactivation rate associated with the increased k_{I1I2} (Fig. 8 *C*). The sum of these latter two effects of 5HT resulted in an overall slight increase in the macroscopic inactivation rate (Fig. 8 *D*). Note that the relative shapes of the simulated currents in Fig. 8 *D*, which have been normalized regarding peak current, closely resemble the relative shapes of real currents, recorded before and after 5HT treatment and similarly normalized (Fig. 2 *B*).

That a decrease in the rate of inactivation of open channels could result in an increased peak current is easy to understand. Less intuitive is why an increase in k_{I1I2} would increase the inactivation rate. Presumably an increase in k_{I1I2} would increase the number of channels leaving I_{fast} to enter I_{slow}. Inactivated channels residing in I_{slow} could require longer times than I_{fast} and/or might have to first pass through I_{fast}, to revert back to the open state. The depletion of channels in I_{fast}, which is most rapidly converted back to the open state, could result in fewer openings from the inactivated state and increase ratio of channels undergoing inactivation relative to those opening from the inactivated state. This process could disproportionately impact the inactivation rather than the peak amplitude of the current because of the relatively slow rate of transition from I_{fast} to I_{slow}.

The observation that 1-s inactivating CPs antagonized the 5HT induced increase in Na^+ current amplitude can also be explained in terms of the above mentioned simulations. The simulation depicted in Fig. 8 *C* suggests that, under control conditions, reopenings from I_{fast} begin to occur before the current peaks and contribute significantly to the peak Na^+ current. Thus, we hypothesize that the interaction of the 5HT increased k_{I1I2} with the 1-s inactivation pulse enhances the depletion of the pool of channels in I_{fast}, due to an increase in the number of channels that undergo transition to I_{slow}. Consequently, the pool of channels in I_{fast}, available to reopen and participate in the peak current, would be reduced to a larger degree in the presence of 5HT than under control conditions. Thus, after a 1-s inactivation pulse, a decrease in peak current produced by 5HT increased k_{I1I2} could offset the increase in peak current produced by the effect of 5HT on k_{OI1}.

The above hypothesis hinges on the assumption that the increase in k_{I1I2} produced by 5HT would disproportionately interact with 1-s inactivation pulses versus 60-ms or 100-ms inactivation pulses, to deplete the pool of channels in the I_{fast} state. This disproportionate effect might occur because 1-s inactivation pulses allow sufficient time for the transfer of many channels from I_{fast} to I_{slow}. Thus, there would be time for increase of k_{I1I2} by 5HT to significantly enhance this process. On the other hand, the 5HT induced increase in k_{I1I2} may have less impact on the transfer of channels from

I_{fast} to I_{slow} during a 60- or 100-ms inactivation pulse, because fewer channels undergo this transition during these short time periods.

Although we have no direct proof of this hypothesis, some of our electrophysiological data suggest that that 5HT increased the proportion of inactivated channels residing in I_{slow}. The experiments on removal of inactivation suggest that 5HT slowed the rate of removal by shifting inactivated channels into a state that was more slowly removed and that this process was enhanced by long duration CPs. The above putative shifting of inactivated channels may correspond with the 5HT-induced reduction of the more depolarized shoulder (V_{h1}) of the availability curves. These electrophysiological observations are consistent with the results of the modeling suggesting that 5HT increases k_{I1I2}.

In conclusion, our data and computer modeling studies suggest that 5HT increased voltage sensitive TTX-resistant Na^+ conductance in the nociceptor-like type 2 DRG cells by altering channel kinetics. The idea that the predominant changes produced by 5HT are the rates of transition between the open state and an inactivated state is consistent with the observation that inflammatory mediators not only increase Na^+ conductance in nociceptor models, but also increase the rates of activation and inactivation. Similar modeling studies on the decrease in TTX-sensitive Na^+ currents by PKA-dependent channel phosphorylation in rat striatal neurons suggest that, in that case, the underlying mechanism is an increase in the rate of transition between an open state and an inactivated state (d'Alcantara et al., 1999). PKA-dependent phosphorylation of TTX-resistant Na^+ channels is also involved in the increase in Na^+ conductance produced by inflammatory mediators in nociceptors (England et al., 1996; Gold et al., 1998; Cardenas et al., 2001; Fitzgerald et al., 1999). Thus, it may be that changes in the rate of transition between an open state and an inactivated state is a general mechanism by which PKA dependent phosphorylation modulates both TTX-sensitive and TTX-resistant Na^+ channels.

A previous study showing that 5HT induced increases in TTX-resistant Na^+ current significantly increases the excitability of type 2 DRG cells (Cardenas et al., 2001), combined with the present work, suggests that subtle changes in channel gating kinetics can produce profound changes in neuronal behavior. The present study suggests additionally that it may be possible to manipulate TTX-resistant Na^+ channel kinetics to a clinical advantage. Our data indicate that long duration inactivation CPs antagonize the modulation of Na^+ current by 5HT in the nociceptor like type 2 DRG cells. This suggests the possibility that drugs, developed to induce and/or stabilize slow inactivated states of TTX-resistant Na^+ channels, could be useful in reducing hyperalgesia associated with pathological conditions or medical procedures. The antagonism of the 5HT induced increase in Na^+ current by induction of I_{slow} appeared to be related to the proportion of inactivated channels residing in I_{slow} and complete current inactivation was not required. Thus, perhaps a balance could be struck whereby hyperalgesia could be significantly reduced while maintaining a response to normally painful stimuli.

This work was supported by National Institutes of Health grant NS37067 to R. S. Scroggs, the Belgian Program on University Poles of Attraction, FMRE (Neurobiology 99-01), and FRSM-Belgium (3.4551.98). The authors would like to thank Dr. S. N. Schiffmann for support in this work.

REFERENCES

Akopian, A. N., L. Sivilotti, and J. N. Wood. 1996. A tetrodotoxin-resistant voltage-gated sodium channel expressed by sensory neurons. *Nature.* 379:257–262.

Cardenas, L. M., C. G. Cardenas, and R. S. Scroggs. 2001. 5HT increases excitability of nociceptor-like rat dorsal root ganglion neurons via cAMP-coupled TTX-resistant Na^+ channels. *J. Neurophysiol.* 86: 241–248.

Cardenas, C. G., L. P. Del Mar, B. Y. Cooper, and R. S. Scroggs. 1997. $5HT_4$ receptors couple positively to tetrodotoxin-insensitive sodium channels in a subpopulation of capsaicin sensitive rat sensory neurons. *J. Neurosci.* 17:7181–7189.

Cardenas, C. G., L. P. Del Mar, and R. S. Scroggs. 1995. Variation in serotonergic inhibition of calcium channel currents in four types of rat sensory neurons differentiated by membrane properties. *J. Neurophysiol.* 74:1870–1879.

d'Alcantara, P., S. N. Schiffmann, and S. Swillens. 1999. Effects of protein kinase A-induced phosphorylation on the gating mechanism of the brain Na^+ channel: model fitting to whole-cell current traces. *Biophys. J.* 77:204–216.

Del Mar, L. P., and R. S. Scroggs. 1996. Lactoseries carbohydrate antigen, Galβ1–4GlcNAc-R, is expressed by a subpopulation of capsaicin-sensitive rat sensory neurons. *J. Neurophysiol.* 76:2192–2199.

Dodd, J., and T. M. Jessell. 1985. Lactoseries carbohydrates specify subsets of dorsal root ganglion neurons projecting to the superficial dorsal horn of rat spinal cord. *J. Neurosci.* 5:3278–3294.

England, S., S. Bevan, and R. J. Docherty. 1996. PGE_2 modulates the tetrodotoxin-resistant sodium current in neonatal rat dorsal root ganglion neurones via the cyclic AMP-protein kinase cascade. *J. Physiol.* 495:429–440.

Fernandez, J. M., A. P. Fox, and S. Krasne. 1984. Membrane patches and whole-cell membranes: a comparison of electrical properties in rat clonal pituitary (GH_3) cells. *J. Physiol.* 356:565–585.

Fitzgerald, E. M., K. Okuse, J. N. Wood, A. C. Dolphin, and S. J. Moss. 1999. cAMP-dependent phosphorylation of the tetrodotoxin-resistant voltage-dependent sodium channel SNS. *J. Physiol.* 516:433–446.

Gold, M. S., J. D. Levine, and A. M. Correa. 1998. Modulation of TTX-R I_{Na} by PKC and PKA and their role in PGE_2 induced sensitization of rat sensory neurons in vitro. *J. Neurosci.* 18:10345–10355.

Gold, M. S., D. B. Reichling, M. J. Shuster, and J. D. Levine. 1996. Hyperalgesic agents increase a tetrodotoxin-resistant Na^+ current in nociceptors. *Proc. Natl. Acad. Sci. U. S. A.* 93:1108–1112.

Goldman, L. 1995. Sodium channel inactivation from closed states: evidence for an intrinsic voltage dependency. *Biophys. J.* 69:2369–2377.

Harper, A. A., and S. N. Lawson. 1985a. Conduction velocity is related to morphological cell type in rat dorsal root ganglion neurones. *J. Physiol.* 359:31–46.

Harper, A. A., and S. N. Lawson. 1985b. Electrical properties of rat dorsal root ganglion neurons with different peripheral nerve conduction velocities. *J. Physiol.* 359:47–63.

Hille, B. 1992. Ionic Channels in Excitable Membranes. Sinauer Associates, Inc, Sunderlan, MA. 457–461.

Holzer, P. 1991. Capsaicin: cellular targets, mechanisms of action, and selectivity for thin sensory neurons. *Pharmacol. Rev.* 43:143–201.

Light, A. R., and E. R. Perl. 1976. Spinal termination of functionally identified primary afferent neurons with slowly conducting myelinated fibers. *J. Comp. Neurol.* 186:133–150.

Light, A. R., and E. R. Perl. 1979. Re-examination of the dorsal root projection to the spinal dorsal horn including observations on the differential termination of course and fine fibers. *J. Comp. Neurol.* 186:117–132.

Roy, M. L., and T. Narahashi. 1992. Differential properties of tetrodotoxin-sensitive and tetrodotoxin-resistant sodium channels in rat dorsal root ganglion neurons. *J. Neurosci.* 12:2104–2111.

Rush, A. M., M. E. Brau, A. A. Elliott, and J. R. Elliot. 1998. Electrophysical properties of sodium current subtypes in small cells from adult rat dorsal root ganglia. *J. Physiol.* 511:771–789.

Scroggs, R. S., and A. P. Fox. 1992. Calcium current variation between acutely isolated adult rat dorsal root ganglion neurons of different size. *J. Physiol.* 445:639–658.

Taiwo, Y. O., P. H. Heller, and J. D. Levine. 1992. Mediation of serotonin hyperalgesia by the cAMP second messenger system. *Neuroscience.* 48:479–483.

Taiwo, Y. O., and J. D. Levine. 1992. Serotonin is a directly-acting hyperalgesic agent in the rat. *Neuroscience.* 48:485–490.

Vandenberg, C. A., and F. Bezanilla. 1991. A sodium channel-gating model based on single channel macroscopic ionic, and gating currents in the squid giant axon. *Biophys. J.* 60:1511–1533.

Villiere, V., and E. M. McLachlan. 1996. Electrophysiological properties of neurons in intact rat dorsal root ganglia classified by conduction velocity and action potential duration. *J. Neurophysiol.* 76:1924–1941.

Yakehiro, M., T. Yuki, K. Yamaoka, T. Furue, Y. Mori, K. Imoto, and I. Seyama. 2000. An analysis of the variations in potency of grayanotoxin analogues in modifying frog sodium channels of differing subtypes. *Mol. Pharmacol.* 58:692–700.